16th European Signal Processing Conference (EUSIPCO 2008), Lausanne, Switzerland, August 25-29, 2008, copyright by EURASIP

# EQUIDISTRIBUTED SEQUENCES ALONG SPACE-FILLING CURVES IN SAMPLING OF IMAGES

*Ewaryst Rafajłowicz, Ewa Skubalska-Rafajłowicz*

Institute of Computer Eng., Control and Robotics, Wrocław University of Technology
Wybrzeże Wyspiańskiego 27, 50 370, Wrocław, Poland
+(48 71) 320 27 95, ewaryst.rafajlowicz@pwr.wroc.pl

## ABSTRACT

A new sampling scheme for 2D images is proposed, which is dedicated for fast processing and storing long sequences of industrial images. It was proved that the spectrum of non-bandlimited images can be approximated up to a desired accuracy when number of samples grows. A simple reconstruction scheme is also proposed.

## 1. INTRODUCTION

We propose a new sampling scheme of 2D images, which is obtained from one dimensional equidistributed sequences (EQD sequences), transformed by a space-filling curve (SFC). EQD sequences (see, e.g. [7]) are deterministic sequences $t_1, t_2, \ldots, t_n$, which behave as if they were drawn from the uniform distribution, but they behave more regularly than random samples. Thus image descriptors can be evaluated more exactly (see [10] for account on descriptors).

A space-filling curve is a continuous function, $\Phi(t)$ that maps the unit interval $T = [0,1]$ onto the unit (hyper-)cube, but here we confine our attention to the unit square $I_2 = [0,1]^2$. The Hilbert, Peano and Sierpiński curves provide examples of SFCs (see [11]). For a selected EQD sequence $t_1, t_2, \ldots, t_n$ we shall generate sample points $x_1, t_2, \ldots, x_n$ as follows $x_i = \Phi(t_i)$, $i = 1, 2, \ldots, n$. Advantages of this sampling scheme, considered from a view point of processing industrial images (see [4] for the state) are the following.
1) Gray levels at sample points remain unchanged. This allows for the analysis of defects in products, keeping storage requirements for archiving at a reasonable level.
2) Image descriptors can be evaluated with a low computational burden.
3) The Fourier spectra of images can be approximated with a desired accuracy.
4) Original images can be relatively quickly and reliably reconstructed (in fact approximated) from samples.
5) Samples are linearly ordered, preserving closeness in the sense that points, which are closely sampled along SFC are also close in the underlying image.
Note that 2D and multidimensional EQD sequences are well known (see, e.g., [7]), the Halton and Hammersley sequences being the most popular. They are generated directly, without using SFC. They can also be used for sampling images, but then we loose advantages 4) and 5).

Earlier results on applying SFCs in image processing concentrated mainly on their scanning properties. Here, we additionally use their ability to preserve the Lebesgue measure and closeness of neighbor points. The Shannon's sampling theorem is not applicable here, since images are usually not band-limited. Instead, we describe images by measurable functions, which admit sudden changes of intensities. In recent years one can observe a renewed interest of researchers in studying image sampling (see [18], where Shannon's theorem is generalized to non-bandlimited functions and [1], [17], [3] for recent contributions).

## 2. PRELIMINARIES

Let $f(x)$ denote gray levels of an image at $x \in I_2$. We admit images $f : I_2 \to [0,1]$ to be from the space of the Lebesgue measurable functions (see, e.g., [19]), which include discontinuous functions.

**Remark 2.1** *By the Lusin theorem [19], for every $\varepsilon > 0$ there exists set $E(\varepsilon)$ such that $\mu_2(I_2 - E(\varepsilon)) < \varepsilon$ and $f$ restricted to this set, further denoted as $f|_E$, is continuous.*

**EQD sequences.** A deterministic sequence $(x_i)_{i=1}^n$ is called EQD (or uniformly distributed) sequence in $I_d \stackrel{def}{=} [0,1]^d$ if

$$\lim_{n\to\infty} n^{-1} \sum_{i=1}^{n} g(x_i) = \int_{I_d} g(x)dx$$

holds for every continuous function $g$ on $I_d$ (see, e.g. [7]). We shall use this definition for $d = 1$ and $d = 2$. The well known way of generating EQD sequences in $[0, 1]$ is as follows

$$t_i = \text{frac}(i\,\theta), \qquad i = 1, 2, \ldots, \quad (1)$$

where the fractional part is denoted as frac(.), $\theta$ is an irrational number.

**Space-filling curves** A space-filling curve is a continuous mapping $\Phi : I_1 \stackrel{onto}{\to} I_d$. The well known curves constructed by Hilbert, Peano and Sierpiński possess the following properties (see [11], [8], [9], [12]):

F1) for every continuous function $g : I_2 \to R$

$$\int_{I_2} g(x)\,dx = \int_0^1 g(\Phi(t))dt, \qquad (2)$$

where $x = [x^{(1)}, x^{(2)}]^T$ and $T$ denotes the transposition,

F2) there exists $C_\Phi > 0$ such that

$$||\Phi(t) - \Phi(t')|| \le C_\Phi |t - t'|^{1/2}, \quad (3)$$

where $||.||$ is the Euclidean norm in $R^2$. The Lipschitz continuity (3) is stated above for 2D case and it reads intuitively as distance preserving property in the sense that points close to each other in the interval are transformed by $\Phi$ onto points close together in $I_2$, but the converse is not necessarily true. The reason is in that $\Phi$ does not have the inverse (see [11]) in the usual sense (intuitively, because a curve intersects itself). For our purposes it is of interest to find at least one $t \in I_1$ such that $\Phi(t) = x$ for given x. Consider a transformation $\Psi : I_2 \to I_1$, such that $\Psi(x) \in \Phi^{-1}(x)$, where $\Phi^{-1}(x)$ denotes the inverse image of $x$, i.e., the set $\{t \in I_1 : \Phi(t) = x\}$. $\Phi^{-1}$ allows to order linearly pixels in an image. We shall call $\Psi$ a quasi-inverse of $\Phi$.

F3) $\Phi$ is the Lebesgue measure preserving in the sense that for every Borel $A \subset I_2$ we have $\mu_2(A) = \mu_1(\Phi^{-1}(A))$, where $\mu_1$ and $\mu_2$ denote the Lebesgue measure in $R_1$ and $R_2$, respectively.

F4) One can construct a quasi-inverse $\Psi$ in such a way that it is also Lebesgue measure preserving.

**Remark 2.2** *It is important that for the Peano, Hilbert and Sierpiński curves there exist algorithms for calculating their approximate value at a given point $t \in I_1$ with $O\left(\frac{d}{\varepsilon}\right)$ of arithmetic operations, where $\varepsilon > 0$ denotes the accuracy of approximation (see [2], [16], [13]). Furthermore, also quasi-inverses of these curves can be calculated with the same computational complexity (see [14], [15], [13]).*

## 3. SAMPLING SCHEME AND ITS PROPERTIES

The proposed sampling scheme is as follows.

**Step 1)** Calculate $t_i$'s as in (1).
**Step 2)** Calculate $x_i$'s as $x_i = \Phi(t_i)$
**Step 3)** Read out samples $f_i = f(x_i)$, $i = 1, 2, \ldots, n$.

For given $n$ and $\theta$ it suffices to perform Steps 1) and 2) only once.

**Remark 3.1** *The above version of sampling should be slightly modified in practice by recalculating positions of sample points in Step 2), which have coordinates in $I_2$, to coordinates of pixels in a real image, which has $N_h$ pixels width and $N_v$ pixels height. Denote by $(n_h(i), n_v(i))$ the horizontal and vertical coordinates, which correspond to $x_i$. Also gray levels and $f_i$'s are usually stored as integers from* 0 *to* 255 *instead of* $[0, 1]$.

Below we state briefly selected properties of the above sampling scheme, which are of interest in image processing.

**Uniform distribution**

P1) $\{x_i\}_{i=1}^n$, *is EQD sequence in $I_2$.*

For continuous $g : I_2 \to R$, $n^{-1}\sum_{i=1}^n g(x_i) = n^{-1}\sum_{i=1}^n g(\Phi(t_i)) \to \int_0^1 g(\Phi(t))dt = \int_{I_2} g(x)\,dx$, since $t_i \in I_1$ are EQD, $\Phi$ is

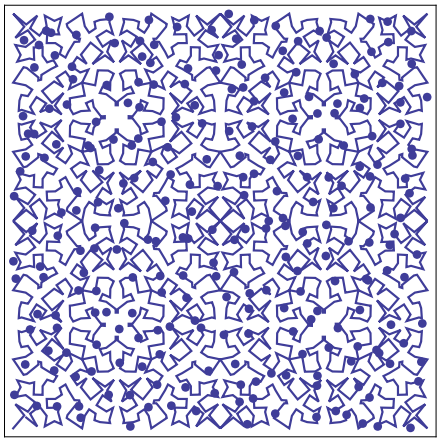

Figure 1: The Sierpiński SFC and $n = 256$ EQD points.

continuous, while the last equality follows from F1).•

**Descriptors** Descriptors $a_k$ with respect to linearly independent and continuous functions $v_k(x)$ are defined as $a_k = \int_{I_2} f(x)\, v_k(x)\, dx,\ k = 1, 2, \ldots$. $a_k$'s are usually approximated by the sums of gray levels located at all the pixels. We can gain much on efficiency using $\hat{\alpha}_k^{(n)} = n^{-1} \sum_{i=1}^{n} f_i$.

P2) $\lim_{n\to\infty} |\alpha_k - \hat{\alpha}_k^{(n)}| = 0$

We omit the proof (see below).

**Spectrum approximation** Denote by $\mathscr{F}(\omega)$, $\omega = [\omega^{(1)}, \omega^{(2)}]^T$ the Fourier transform of image $f$, i.e.,

$$\mathscr{F}(\omega) = \int_{I_2} \exp(-\mathbf{j}\, \omega^T x)\, f(x)\, dx, \quad (4)$$

where $\mathbf{j}^2 = -1$. We approximate $\mathscr{F}$ by

$$\hat{\mathscr{F}}_n(\omega) = n^{-1} \sum_{i=1}^{n} \exp(-\mathbf{j}\, \omega^T x_i)\, f_i. \quad (5)$$

P3) *If $f$ is measurable in $I_2$, then for every $\omega$ we have*

$$\lim_{n\to\infty} \left| \mathscr{F}(\omega) - \hat{\mathscr{F}}_n(\omega) \right| = 0. \quad (6)$$

Take arbitrary $\varepsilon > 0$. By the Lusin thm., there exists a set $E = E(\varepsilon/4)$ such that $f|_E$ is continuous and $\mu_2(E - I_2) < \varepsilon/4$. Denote by $\mathscr{F}_E(\omega)$ the Fourier transform of $f|_E$. Then, for $D \stackrel{def}{=} E - I_2$

$$|\mathscr{F}(\omega) - \mathscr{F}_E(\omega)| = \left| \int_D e^{-\mathbf{j}\,\omega^T x} f(x)\, dx \right| < \mu_2(D) < \frac{\varepsilon}{4}, \quad (7)$$

since both integrands do not exceed 1. Let

$$\hat{\mathscr{F}}_E(\omega) = n^{-1} \sum_{x_i \in E} \exp(-\mathbf{j}\, \omega^T x_i)\, f_i. \quad (8)$$

Define $\Delta_n = \left| \hat{\mathscr{F}}_n(\omega) - \hat{\mathscr{F}}_E(\omega) \right|$. Then

$$\Delta_n = \left| n^{-1} \sum_{x_i \notin E} \exp(-\mathbf{j}\, \omega^T x_i)\, f_i \right|. \quad (9)$$

Clearly, $\Delta_n \le n(I_2 - E)/n$, where

$$n(I_2 - E) \stackrel{def}{=} \mathrm{card}\{i : x_i \in (I_2 - E)\}.$$

From P1) it follows that for $n \to \infty$

$$\Delta_n \le \frac{n(I_2 - E)}{n} \to \mu_2(I_2 - E) < \varepsilon/4. \quad (10)$$

Thus, for $n$ sufficiently large we have $\Delta_n < \varepsilon/4$. Define

$$\delta_n = \left| \left( \frac{1}{n} - \frac{1}{n(E)} \right) \sum_{x_i \in E} \exp(-\mathbf{j}\, \omega^T x_i)\, f_i \right|$$

where $n(E) \stackrel{def}{=} \mathrm{card}\{i : x_i \in E\}$. Clearly,

$$\left| \sum_{x_i \in E} \exp(-\mathbf{j}\, \omega^T x_i)\, f_i \right| \le n(E).$$

Thus, for $n$ large enough

$$\delta_n \le |(n(E)/n - 1|) < \varepsilon/4, \quad (11)$$

since, by P1), $|(n(E)/n - \mu_2(I_2)|) \to 0$ as $n \to \infty$. We omit argument $\omega$ in he formulas that follow. Summarizing, we obtain.

$$\left| \mathscr{F} - \hat{\mathscr{F}}_n \right| < \varepsilon/4 + \left| F_E - \hat{\mathscr{F}}_n \right|, \quad (12)$$

since, by (7), $|\mathscr{F} - \mathscr{F}_E| < \varepsilon/4$. Analogously,

$$\left| \mathscr{F}_E - \hat{\mathscr{F}}_n \right| < \varepsilon/4 + \left| \hat{\mathscr{F}}_E - \hat{\mathscr{F}}_n \right|, \quad (13)$$

due to (10). Finally,

$$\left| \mathscr{F}_E - \hat{\mathscr{F}}_E \right| \le \delta_n + \quad (14)$$

$$+\left|\mathscr{F}_E - n_E^{-1}\sum_{x_i\in E}\exp(-\mathbf{j}\,\omega^T x_i)\,f_i\right|.$$

The last term in (14) approaches to zero, since $f$ is continuous in $E$ and P1) holds. Hence, $\left|\mathscr{F}_E-\hat{\mathscr{F}}_E\right| < \varepsilon/2$ for $n$ large enough, due to (11). Using this inequality in (13) and invoking (12) we obtain that for $n$ large enough we have $\left|\mathscr{F}-\hat{\mathscr{F}}_n\right| < \varepsilon.\bullet$

A detailed discussion of the convergence rate of $\hat{\mathscr{F}}_n(\omega)$ to $\mathscr{F}(\omega)$ is outside the scope of this paper. We only mention that if for $f$ the Lipschitz condition with the exponent $0<\alpha\le 1$ holds, then

$$\left|\mathscr{F}(\omega)-\hat{\mathscr{F}}_n(\omega)\right| \le C\,(log(n)/n)^{\alpha/2},$$

where $C>0$ is a constant, which may depend on $f$, SFC and $\omega$, but not on $n$.

**A remark on segmentation** Assume that sample points $(t_i, f_i)$, $i=1,2,\ldots,n$ are reordered according to their first coordinates, i.e., $(t_{(i)}, f_{(i)})$, $t_{(i)} < t_{(i+1)}$. Our aim is to mark (approximately) regions such that

$$\{x\in I_2 : T_1 < f(x) < T_2\}, \qquad (15)$$

where $0\le T_1 < T_2 \le 1$ are specified thresholds. Varying $T_1$ and $T_2$ one can obtain approximate segmentation of the image. The segmentation task is time consuming. We can reduce the computational burden as follows. Suppose that for a certain cluster of points $t_{(p)}, t_{(p+1)},\ldots,t_{(q)}$ we have $T_1 < f_{(j)} < T_2$, $j=p, p+1,\ldots,q$. Then, according to F2), also points $x_{(j)}=\Phi(t_{(j)})$ are close in the image and form a cluster. Furthermore, according to F3) and F4), the length $\left|t_{(q)}-t_{(p)}\right|$ can be used as an approximation of the area of the smallest polygon containing $x_{(j)}$, $j=p,p+1,\ldots,q$.

## 4. RECONSTRUCTION BY (NEAREST) NEIGHBOR TECHNIQUE

Our aim is to demonstrate that images can be efficiently reconstructed from the samples. Consider $N_h\times N_v$ image. The coordinates of its pixels are denoted as $(k,m)$, while positions of sample points are denoted as $(n_h(i), n_v(i))$, $i=1,2,\ldots,n$. Abusing the notation, we shall write $f_{(k,m)}$, forgetting for a while that earlier $f$ was defined in $[0,1]^2$.

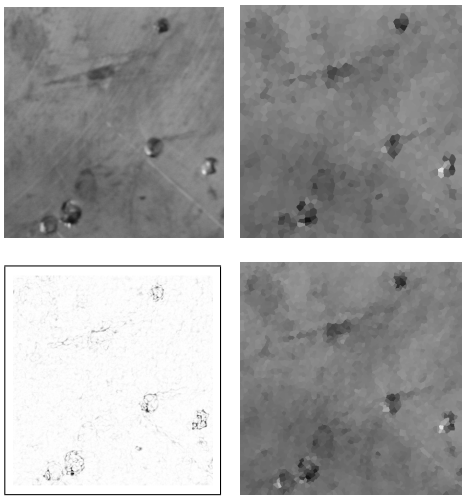

Figure 2: Upper left panel – an original $10^3\times 10^3$ image of a defected copper slab. Reconstruction from $n=2048$ samples (upper right) and from $n=4096$ samples (lower right). Lower left panel – the difference between the original image and its reconstruction from $n=4096$ samples.

A naive algorithm of reconstructing the underlying image would be the following. Find the nearest neighbor (NN) of $(k,m)$ among $(n_h(i), n_v(i))$'s and extend the gray level of the neighbor to $(k,m)$ pixel. Repeat the above to for all $N_hN_v$ pixels. This approach is too time consuming, since the search of NN among $n$, which is about $10^4$, in 2D, multiplied by an image resolution (typically 3-8 MPix).

Assume that $t_{(i)}$, $i=1,2,\ldots,n$ are ordered. The proposed method is as follows.

**Step 1** Normalize current pixel $(k,m)$ to $I_2$ as $x_{km}\stackrel{def}{=}(k/N_h, m/N_v)$.

**Step 2** Calculate $t_{km}\stackrel{def}{=}\Psi(x_{km})$

**Step 3** Find its NN among all $t_{(i)}$'s. Denote its number by $i(km)$.

**Step 4** As the approximate value of $f$ at pixel $(k,m)$ (or at $x_{km}$) take $f$ at $(n_h(i(km)), n_v(i(km)))$ (or $f(x_{i(km)})$).

**Step 5** Repeat Steps 1-4 for all $(k,m)$.

The main advantage of this scheme is in that finding NN among ordered $t_{(i)}$'s has computational complexity $O(\log_2(n))$. The price for that is a possibility of missing the true NN in $I_2$, since in Step 2 we use the

quasi-inverse of SFC. Nevertheless, a point found in Step 3 is close to NN in $I_2$ due to F2). The results of reconstructing of a real image are shown in Fig. 2.

## 5. CONCLUDING REMARKS

Taking into account the simplicity of the sampling scheme and NN reconstruction, one can hope that the proposed method, combined with the techniques loss-less compression provides sufficiently good compression rates for storing samples of long sequences of industrial images, without loosing original gray levels and other features, which are essential for detecting defects and reasons of their occurrence.

The method applies to color images in RGB format just by repeating it each color separately. The search for NN is done only once for each pixel.

## REFERENCES


[1] Anton F., Mioc D., Fournier A., Reconstructing 2D images with natural neighbour interpolation, The Visual Computer, 17, 134-146, 2001.

[2] Butz A.. Alternative Algorithm for Hilbert's Space-filling Curve, IEEE Trans. on Computing, vol. C-20, 424–426, 1971.

[3] Cohen A., Merhav N., Weissman T., Scanning and sequential decision making for multidimensional data Part I: The noiseless case, IEEE Trans. Information Th., vol. 53, 3001-3020, 2007.

[4] Davies, E.R. *Machine Vision*, Morgan Kaufmann, 2005.

[5] Davies, E.R., A sampling approach to ultra-fast object location, Real-Time Imaging 7, no. 4, 339-355, 2001.

[6] Davis P., Rabinowitz P. *Methods of Numerical Integration.* Academic Press, 1984.

[7] Kuipers L., Niederreiter H. *Uniform Distribution of Sequences.* Wiley, 1974.

[8] Milne S. C. Peano curves and smoothness of functions. *Advances in Mathematics*, 35:129–157, 1980.

[9] Moore E.H., On certain crinkly curves, Trans. Amer. Math. Soc. 1, 72–90, 1900.

[10] Pawlak M., *Image Analysis by Moments*, Politech. Wrocławska, 2006.

[11] Sagan H., *Space-filling Curves*, Springer 1994.

[12] Sierpiński W. Sur une nouvelle courbe continue qui remplit toute une aire plane. *Bull. de l'Acad. des Sci. de Cracovie A.*, 463–478, 1912.

[13] Skubalska-Rafajłowicz E., Pattern recognition algorithms based on space-filling curves and orthogonal expansions. IEEE Trans. Information Th., vol. 47, pp 1915-1927, 2001.

[14] Skubalska-Rafajłowicz E.: Recurrent network structure for computing quasi-inverses of the Sierpiński space-filling curves. Lect. Notes in Comp. Sci. Springer 3070, 272–277, 2004.

[15] Skubalska-Rafajłowicz E.: Data compression for pattern recognition based on space-filling curve pseudo-inverse mapping. *Nonlinear Analysis*. vol. 47, 315–326, 2001.

[16] Skubalska-Rafajłowicz Ewa.: Neural networks with orthogonal activation function approximating space-filling curves. Proc. 9th IEEE Int. Conf. Methods and Models in Automation and Robotics. Miedzyzdroje, Vol. 2, 927–934, 2003.

[17] Someya T., Yokokawa T., Kamada M, Reconstruction of images from their observation through Bayer and honeycomb color filter arrays. Proc. EUSIPCO (TuePmOR6) 2004.

[18] Unse M., Zerubia J., A generalized sampling theory without band-limiting constraints, IEEE Trans. Circ. Syst. II, Vol. 45, 959-969, 1998.

[19] Wheeden R., Zygmund A., *Measure and Integral*, Marcell Dekker, 1977.


**Acknowledgements.** Paper supported by R&D grant 2007-2009 from Ministry of Science and Higher Education of Poland and by the Polish Foundation for Science.